J Mater Sci (2010) 45:2071–2079
DOI 10.1007/s10853-009-3801-4

HTC2009

Wetting and interactions of Ni- and Co-based superalloys with different ceramic materials

F. Valenza · M. L. Muolo · A. Passerone

Received: 25 June 2009 / Accepted: 7 August 2009 / Published online: 25 August 2009

Abstract In this work, a systematic study of the wetting behavior of two Ni-based and one Co-based superalloys, used, in particular, for the fabrication of turbine blades, is presented with reference to different ceramic substrates: sapphire, polycrystalline alumina, zirconia, and mullite. Wettability tests have been performed by means of the "sessile drop" method at 1500 °C; the characterization of the interfaces between the molten drop and the substrates has been performed by SEM/EDS analysis in order to check the final characteristics of the solidified interfaces. The results are discussed in terms of chemical interactions in relation to the processing parameters and as a function of the surface and interfacial, morphological and energetic properties of the systems.

Introduction

The superalloys, especially nickel or cobalt based, have been used for over 50 years for producing blades and vanes in aircraft and land-based gas turbines. At present, gas industrial turbines need improved characteristics such as higher inlet temperature (>1300 °C), higher life time (25000–50000 h) and lower amount of compressor air in order to increase efficiency [1, 2]. The improvement of the process parameters led to an improvement of the composition of superalloys (addition of new solutes) and of the manufacturing technologies involved in the investment casting process of turbine blades. This process, already well known from antiquity as lost wax process, needs the presence of a mold material and of a core material which allows forming the internal cooling channels. Thus, in particular, the knowledge is required of the interactions between these ceramic materials and the molten superalloys in order to minimize the formation of internal defects, to improve the external surface and to reduce time and money consuming operations of finishing after casting [3].

In the literature some papers appeared aimed at investigating interfacial interactions and wetting mechanisms in nickel or cobalt based superalloys with oxides with reference to casting process [4–6]; such kind of studies are also devoted to investigate the possibility of developing heat-resistant oxide fiber reinforced composites [7, 8] or joining processes involving these materials [9–11].

The purpose of this work is to provide a systematic study of the wetting and interfacial behavior of CMSX486 (Ni based), IN738LC (Ni based), and ECY768 (Co based) superalloys, used for the fabrication of turbine blades, with reference to different ceramic substrates: sapphire, polycrystalline alumina, zirconia, and mullite. Sapphire represents a "simple" and ideal case adopted for better understanding the basic phenomena involved in solid–liquid contact, while mullite, which is often the main component for shell or core materials, could be considered as the transition between the smooth and pure oxides used in this work and the rough materials used in factory for investment casting.

Experimental part

Materials

Three different industrial alloys were used for this work: two nickel based (CMSX486 and Inconel 738LC) and one

F. Valenza · M. L. Muolo · A. Passerone (✉)
Institute for Energetics and Interphases (IENI), National Research Council (CNR), 6 via de Marini, 16149 Genoa, Italy
e-mail: a.passerone@ge.ieni.cnr.it

Table 1 Chemical composition of the alloys used for wetting experiment

Material	Composition (at.%)													
	Ni	Co	Cr	C	Al	Ti	W	Ta	Hf	Re	Mo	Si	Mn	Nb
CMSX486	Balance	9.68	5.66	0.36	13.95	0.90	2.87	1.52	0.41	0.99	0.45	–	–	–
IN738LC	Balance	8.19	17.29	0.52	7.28	4.11	0.77	0.53	–	–	1.11	Traces	Traces	0.57
ECY768	10.05	Balance	27.05	3.04	0.47	0.27	2.34	1.24	–	–	–	Traces	Traces	–

cobalt based (ECY768), whose compositions are given in Table 1. Small samples with mass approximately 0.5 g were obtained and polished in order to remove any trace of oxides on the surface.

Wettability tests were performed on four different ceramic substrates: sapphire (maximum impurity level <69 ppm, cut along the basal 0001 plane, optically polished with average roughness measured by AFM, $R_a = 2$ nm and annealed for 2 h at 1100 °C under a vacuum), polycrystalline alumina ($R_a = 0.03$ μm), polycrystalline zirconia (stabilized by yttria 3 wt%, $R_a = 0.03$ μm), and mullite (supplied by Nabaltec as pellets, open porosity 1–3%, sintering temperature 1800 °C, mullite >98%; the pellets have been cut and then polished on SiC paper, to a final roughness $R_a \approx 1$ μm).

All materials have been carefully cleaned by chemical means in an ultrasonic bath just prior to each experiment.

Procedure

The wetting was evaluated by contact angle and drop dimension (height and base diameter) measurements using the sessile drop technique [12] in conjunction with the ad hoc designed ASTRAView image analysis software, which allows surface tension, drop dimensions, and contact angle data to be obtained during each experimental run [13, 14].

Experiments were performed in a specially designed furnace which can reach 1600 °C. It is made of two concentric, horizontal, alumina tubes connected to a high vacuum system. Between the two tubes a constant flux of argon guarantees that, even in the temperature range up to 1600 °C, oxygen does not diffuse inside the experimental chamber. The pressure inside the inner tube can be kept $<10^{-4}$ Pa by a turbomolecular pump; alternatively, controlled atmospheres can be introduced inside the working chamber. The oxygen partial pressure of the working atmosphere is continuously monitored by solid state oxygen sensors at the chamber inlet and outlet.

Temperature is read by a type S thermocouple, placed just below the test specimen, which was calibrated against the melting point of Au, Cu, Ni, and Fe slabs placed in the same place of the test specimens. The precision of the temperature readings can be estimated in ±5 °C.

All the experimental set up is carefully aligned and the drop/substrate couples are recorded as sharp, back-lit images, using a high resolution CCD camera. The drops' profiles are acquired, stored, and then elaborated off-line. The drop/substrate profile can be calculated with a precision of ±1 μm through a careful determination of the magnification factor while the intrinsic precision of contact angle data is of the order of ±0.5°; however, possible optical distortions due to the high temperature involved lead to uncertainties in the measured profiles with a final contact angle accuracy of the order of ±2° [15].

The metal/ceramic couple is introduced by a magnetically operated push rod into the preheated furnace only when all parameters (T, P_{O_2}) reach equilibrium; the time necessary to complete the melting process is of the order of 30 s. After tests, the couple is moved into the colder part of the experimental set without opening it, where it is cooled down to room temperature.

For this work, sessile drops were kept in the furnace for 60 min at 1500 °C under Ar + 5% H_2 atmosphere at 1.1×10^5 Pa (slight over pressure) and the specimens were wrapped by a zirconium getter in order to further reduce the oxygen content in atmosphere. In fact, the oxygen partial pressure measured by the sensors was of the order $P_{O_2} = 10^{-18}$ Pa at 700 °C; the water equilibrium reaction would raise the P_{O_2} value to 10^{-5} Pa at 1500 °C if no Zr getters are used. The presence of Zr getters should set a theoretical minimum oxygen partial pressure of 10^{-18} Pa, i.e., the equilibrium dissociation pressure of ZrO_2.

After tests, the interfacial zones were observed and analyzed by optical and electron microscopy (SEM) coupled with energy dispersive spectroscopy (EDS) analysis.

Results and discussion

The wetting behavior of the three alloys on the ceramic substrates is summarized in Fig. 1. For all the systems the final contact angle is achieved just after melting and is stable with time except for the CMSX486 and ECY768-mullite couples.

The results are reported and discussed here for each liquid metal system; rupture of the substrates, together with removal of fragments strongly adhered to the solidified

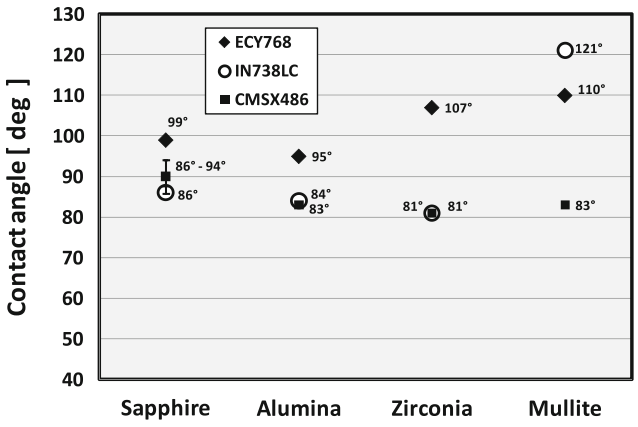

Fig. 1 Wetting data for superalloys-ceramic couples (obtained after 60 min of test)

drop, occurred during cooling because of the residual stresses between the alloy and the ceramic which exceed the "adhesion strength" between the two materials.

CMSX486-ceramic systems

The contact angles which were obtained for CMSX486-oxide systems are reported in Fig. 1; as explained in the following, the contact angles vary between 86° and 94° using sapphire as a substrate while for other systems, angles are below the "formal" limit of wettability: 83° for CMSX486-alumina and mullite substrates and 81° for zirconia.

The following figures show some example of microstructures of the sapphire and alumina substrates: in both cases a thin layer of HfO_2 has been revealed by EDS analysis. For sapphire, stresses during cooling lead to the rupture of the substrate (Fig. 2) while for the less brittle alumina all tests revealed the formation of a continuous, circular crack following the triple line all around (Fig. 3). Even if it was not possible to obtain undamaged solidified samples, the presence of fragments of sapphire still adhering to the solidified drop allowed to cross section the sample and to demonstrate that the thickness of the HfO_2 layer is less than 1 μm (Fig. 4).

For the CMSX486-sapphire system and to a much lesser extent for CMSX486-alumina system, one cannot define uniquely the contact angle; in fact, after melting, the liquid reaches a contact angle of 86° then a cyclic phenomenon has been evidenced: the drop, suddenly and in one step, de-wetted the sapphire substrate reaching a maximum average contact angle of 94° to spread again to 86°. This phenomenon recurred with a period of no more than 10 s and it was also accompanied by a change in drop size as shown in Fig. 5 in which the base diameter is plotted vs.

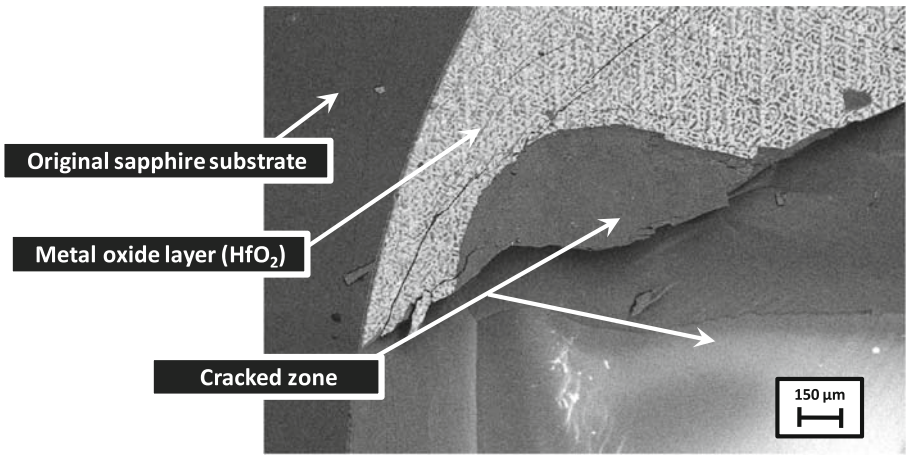

Fig. 2 SEM picture of a sapphire substrate after test with CMSX486 in which a thin HfO_2 layer can be identified adhering to the substrate after drop removal (the rupture of the substrate occurred during cooling)

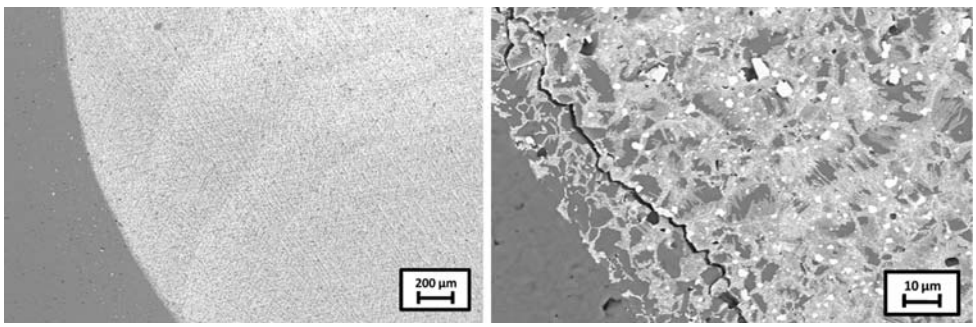

Fig. 3 SEM images of an alumina substrate after test with CMSX486: on the area covered by liquid drop during test, bright zones are visible where HfO_2 was formed during the test. Pictures taken at higher magnification reveal the presence of a continuous, circular crack in correspondence of the triple line

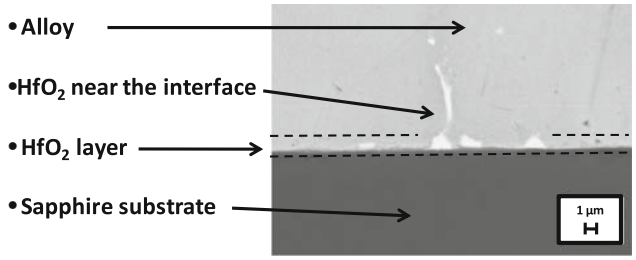

Fig. 4 SEM images of a cross section of a CMSX486-sapphire sample taken in a zone where part of the alloy still adhered to the substrate after cooling. A thin layer and some precipitates of HfO_2 are visible

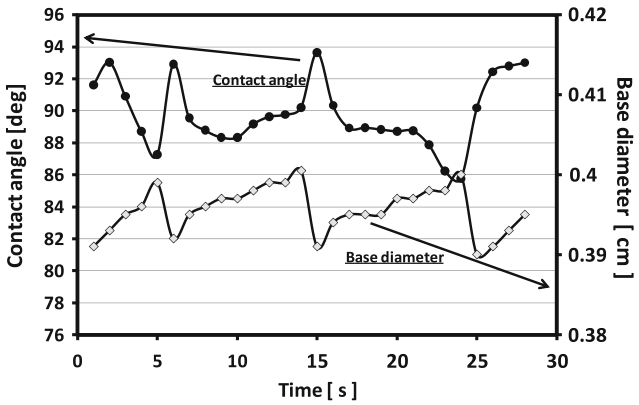

Fig. 5 Contact angle and base diameter plotted as function of time for CMSX486-sapphire system

time. Moreover, erratic movements of the liquid drop along the substrate were found so that new solid–liquid interfaces were formed continuously.

This phenomenon could be justified by the changes in morphology and chemistry of the substrate as well as by a modification of the surface energies; moreover, the movement of the drop could be explained with the presence, at the S/L interface, of gaseous phases involved in the reactions. A similar behavior was reported by Champion et al. [16] or Saiz et al. [17] for the Al–Al_2O_3 system or by Grigorenko et al. [18] for Ni–Al alloys with $X_{Al} > 0.5$ and attributed to liquid evaporation and reaction between the molten metal and the substrate at the triple line accompanied by the formation of the volatile aluminum oxide Al_2O. However, in our case, this explanation does not seem to hold. Indeed, even if Al is present in the superalloy, no special traces like ridges, annular rings, etc. have been found on the ceramic substrate, as no evidence at all of gaseous bubbles escaping from the molten alloy could be found in the recorded images (up to one frame per sec.). A different hypothesis can be invoked. As discussed, Hf segregates at the solid–liquid interface, and its presence as a metallic element should cause a decrease of contact angle. However, due to its higher stability with respect to Al_2O_3, HfO_2 forms at the interface with its own kinetics, making the solid–liquid system to find another equilibrium contact angle, which must be higher due to increase of covalent bonding at the interface. A subsequent further adsorption of Hf, makes the cycle to start again. It may be noted that, as with Ti adsorption at metal-ceramic interfaces, a metallic-like compound more metallic in character like HfO_{2-x} can form just after the Hf adsorption, which also should be wetted by the liquid alloy.

For the CMSX486-zirconia system, in addition to HfO_2, a layer of alumina (thickness 1–2 µm, see Fig. 6) was identified by SEM-EDS; as explained in the following, the formation of alumina is justified by the oxygen coming from reduction of the zirconia substrate.

The CMSX486 on mullite substrate is the only system for which the final contact angle was reached after several minutes (Fig. 7): just after melting, a contact angle of 124° between alloy and substrate was measured but after about 70 s of stability, the angle suddenly decreased down to the final value of 83°. Whiskers also appeared on the edge of the substrate after approximately 30 min. After the tests the drops were found covered by a thin layer of HfO_2. Beneath the oxide layer covering the drop (mainly hafnia) the superalloy appears clean with its usual dendritic structure

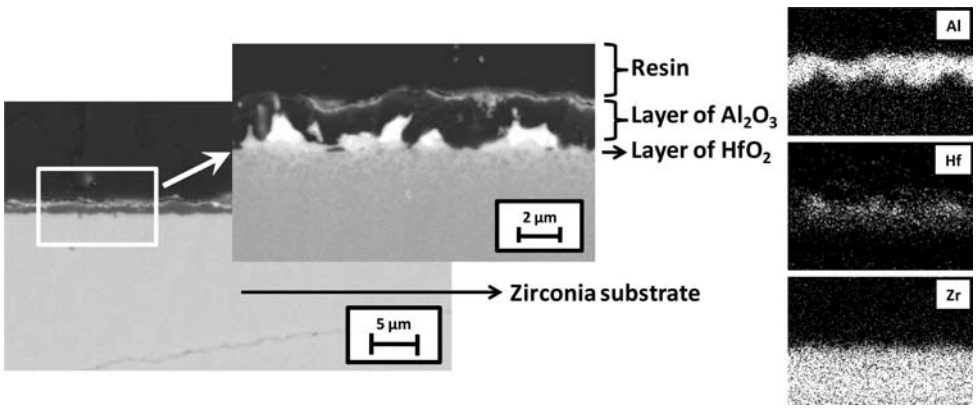

Fig. 6 Layer of HfO_2 and Al_2O_3 at the CMSX486-zirconia interface. On the right, maps indicating the presence of Al, Hf, and Zr at the M/C interface are presented

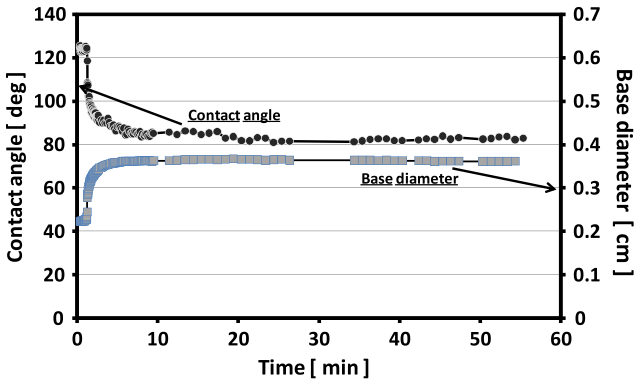

Fig. 7 Contact angle and base diameter plotted as function of time for CMSX486-mullite system

and its standard composition. However, hafnium, which is usually found in the as received alloys as one of the components of the segregated compounds containing high melting elements (Ta, Mo, W, etc.), has not been found at all in the alloy after tests (Fig. 8).

After the tests with CMSX486, different zones appeared on the mullite substrate. As shown in Fig. 9, where the drop was sitting, the substrate is dark because of the formation of a surface layer of HfO_2 (thickness <1 μm); under this, a layer of alumina (thickness ≈ 3 μm) was formed. Outside this area an annular zone appears in the bulk of the substrate constituted by alumina with a higher thickness (≈ 10 μm) and a "spongy" morphology. Elsewhere, just a thin layer of alumina was found to cover the substrate.

IN738LC-ceramic systems

As reported in Fig. 1, the contact angles measured for IN738LC-oxides couples are not very different from those obtained with the CMSX486 alloy: for all systems, except alloy-mullite, contact angles just below 90° have been obtained. However, the interfacial products are mainly influenced by the aluminum content in the alloy (7.3 at.%) more than by other active elements such as chromium (17.3%) or titanium (4.1 at.%).

Similarly to what has been described by other authors [19, 20], alumina crystallites grow on the sapphire substrate at the solid/liquid (S/L) interface and there is formation of grooves on the substrate due to the attack of

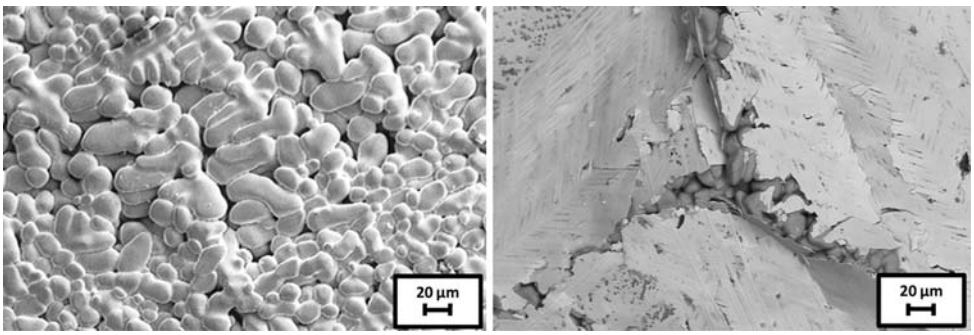

Fig. 8 Top of CMSX486 drops after wetting experiment on zirconia (*left*) and mullite (*right*): for the latter, beneath the oxide crust (HfO_2) the usual morphology of the metallic drop appears

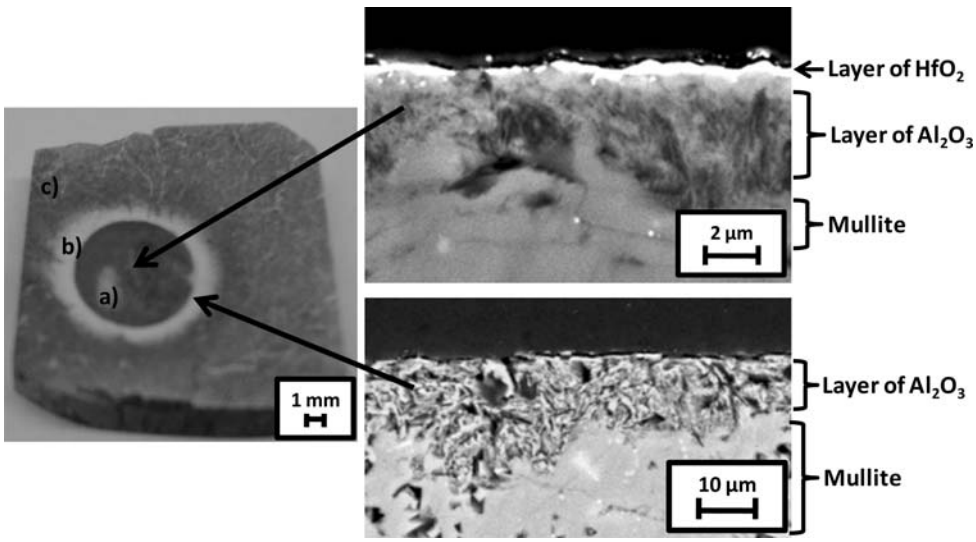

Fig. 9 Mullite substrate after test with CMSX486; on the surface (photographic picture on the left) one can identify three zones: (a) a dark zone where the drop was resting; (b) an anular, white zone all around zone (a); (c) external zone. SEM/EDS analyses made on the cross section of the substrate (on the right) allow identifying composition of the three zones

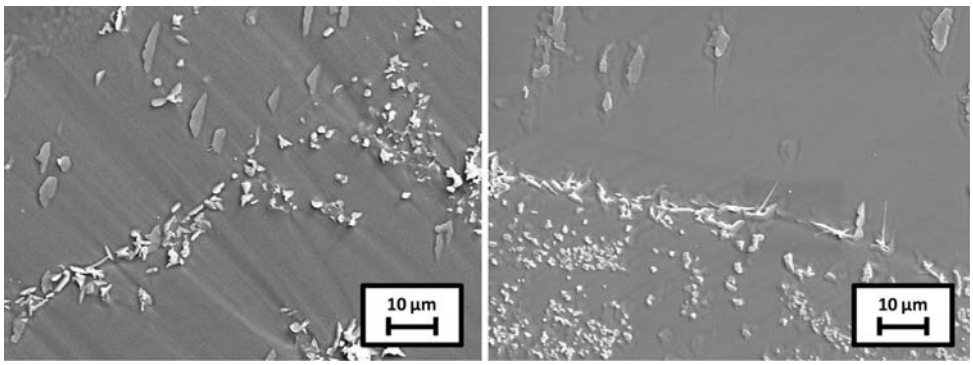

Fig. 10 SEM picture of a sapphire substrate after test with IN738LC: Al_2O_3 crystallites and grooves on the substrate are visible at the former S/L interface

liquid metals like Ni or Al [19, 21, 22] (Fig. 10); the tests performed on polycrystalline substrates did not reveal any important phenomenon except for the presence of a circular crack all around the triple line in the same way as described for CMSX486-alumina system.

For the IN738LC-zirconia substrate, a continuous layer of alumina has been detected at the S/L interface after tests as a consequence of the reduction of the substrate as explained in the following (Fig. 11).

For all tests conducted with mullite, IN738LC oxidized completely after a few minutes from melting; therefore the reported contact angle is valid only for the moments just after melting. A thick layer of Al_2O_3 has been detected by EDS covering the entire drop. Moreover, also in this case, Al_2O_3 forms at the surface of mullite (Fig. 12)

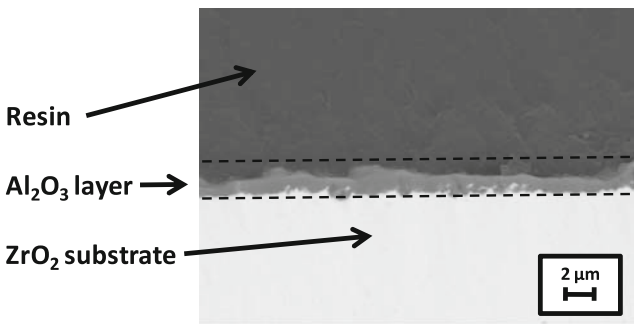

Fig. 11 Cross section of a ZrO_2 substrate after test with IN738LC. A continuous layer of alumina is well visible

ECY768-ceramic systems

For the ECY768 Co-based alloy, a general lower wettability was found: indeed, contact angles (Fig. 1) are always above 90°: starting from 95° obtained with alumina, through the value of 99° for sapphire, and 107° for zirconia, we arrive at 110° obtained with mullite; interfacial compounds have been found but not the presence of evident, continuous layers. As a matter of facts, in comparison to other alloys, ECY768 contains much less active elements and a negligible concentration of aluminum. Anyway, the role played by Hf in CMSX-X tests seems now to be covered by zirconium that, even if present in the alloy at a very low concentration (0.01 at.%), is found as elongated oxide crystals partially embedded at the interface after the tests. This fact is well evidenced in the tests for the ECY768-sapphire couples: during tests on this system, the liquid has moved on the substrate leaving a trail of ZrO_2 precipitates; moreover grooves on the substrate and pits appear at the interface, which should have been formed by the reduction of sapphire by zirconium (Fig. 12).

In the ECY768- alumina and zirconia systems (Fig. 13), which showed a relatively high contact angle, the interface is sharp and the metal strongly adhered to the substrate without leading to the complete breaking of the metal/ceramic (M/C) interface as observed for the other systems.

For the ECY768-mullite couples, the final contact angle has been reached after several minutes. As shown in Fig. 14, the contact angle increases with time. Also in this

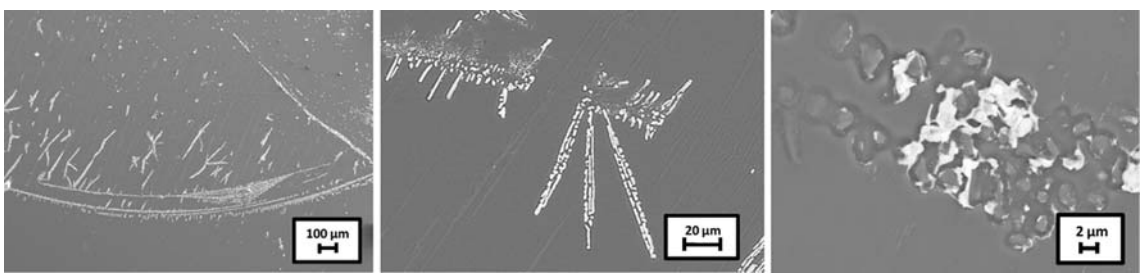

Fig. 12 SEM pictures of a sapphire substrate after test with ECY768: ZrO_2 crystallites and pits are visible at the former S/L interface

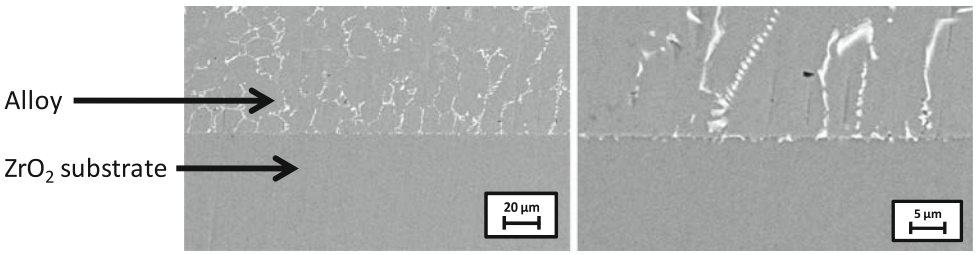

Fig. 13 Cross section of an interface between ECY768 and ZrO_2 after test. White precipitates are formed by segregated heavy elements (W, Ta, Ti)

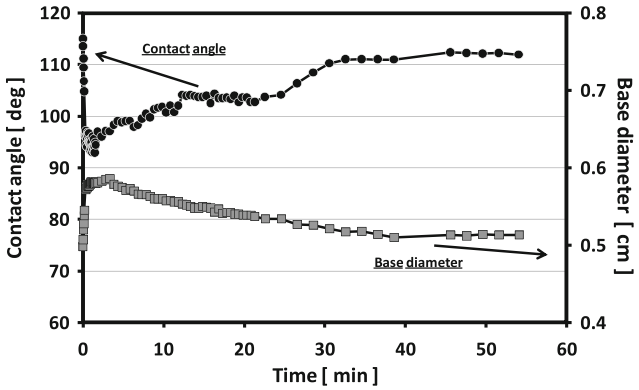

Fig. 14 Contact angle and base diameter plotted as function of time for ECY768-mullite system

case, outside the drop zone, a thick layer of "spongy" alumina was found; moreover, the zone interested by the receding drop is covered by small droplets of the alloy (Fig. 15).

The results already shown demonstrate that the wetting and interfacial phenomena for superalloys-oxide systems are dominated by the presence of active elements also if at low concentrations: the main role is played by hafnium for CMSX486, by aluminum for IN738LC, and by zirconium for ECY768.

However, the presence of chromium at high concentrations in all the alloys calls for further discussion. Its presence in nickel is the topic of several papers discussing the wetting of oxides by Ni as a function of its chromium content [23–25]: even low additions of chromium to pure nickel have been found to increase the wettability without, however, arriving to contact angles below 90°.

Chromium increases the oxygen solubility leading to the formation of Cr–O clusters more active than Ni–O at the interface; these clusters, adsorbing at M/C interface, decrease the S/L interfacial energy [26]. However, in our case, no evidence of chromium enrichment at M/C interface has been found and the interfacial role of chromium is played by other active elements like hafnium, zirconium or aluminum, which have higher affinity for oxygen. Following the three solute approach as in Wan et al. [27], the role of chromium is to increase the activity of these elements in the metal matrix by weakening the interactions between them and the metal matrix.

Moreover, in alloys and superalloys, the high vapor pressure of chromium results, from tests conducted under a vacuum, in a vaporization–condensation process followed by oxidation of chromium due to the residual oxygen partial pressure or to the presence of gaseous SiO if silica containing substrates are used [5, 28]; however, it should be remarked that, just to avoid evaporation, the experiments have been made under a protective, reducing atmosphere, so that no significant evaporation of chromium was found.

As explained before, new oxides are formed at the metal/ceramic interface in form of layers or in form of crystallites depending on the amount of the active metal present in the alloy. The formation of HfO_2 at the interface of CMSX486-X systems is well justified by thermodynamics which assure that formation of this oxide at the expense of Al_2O_3 is the most favorite reaction; in particular for the substrates and some of the alloying elements considered in this work:

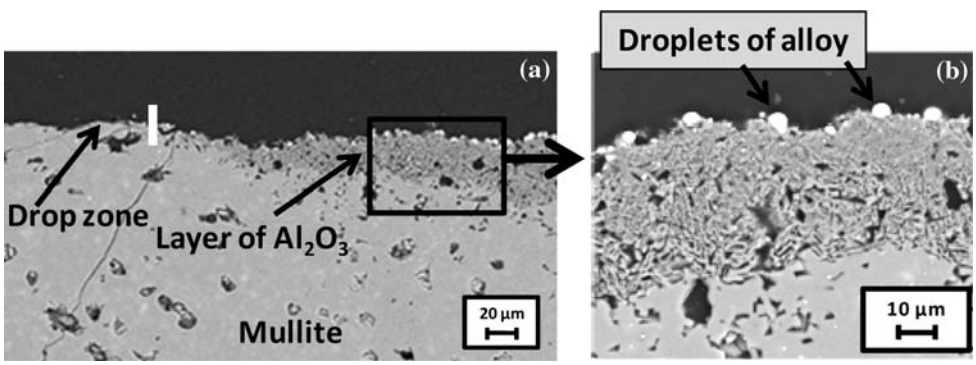

Fig. 15 Cross section of a mullite substrate after test with ECY768. From left to right one can observe: **a** the drop zone (without any reaction) **b** the alumina layer in the bulk with presence of droplets of the alloy

$$Hf + ZrO_2 \leftrightarrow HfO_2 + Zr \quad \Delta G_r^O = -31 \text{ kJ/mol}$$

$$Hf + 2/3Al_2O_3 \leftrightarrow HfO_2 + 4/3Al \quad \Delta G_r^O = -57 \text{ kJ/mol}$$

$$Zr + 2/3Al_2O_3 \leftrightarrow ZrO_2 + 4/3Al \quad \Delta G_r^O = -24 \text{ kJ/mol}$$

calculated at $T = 1500$ °C (thermodynamic data from [29]).

Moreover, when using zirconia as a substrate in our working atmosphere, the oxidation mechanisms are influenced by the reduction of ZrO_2. This process usually occurs by annealing under a vacuum or in reducing atmospheres at high temperatures or because of contact of zirconia with active metals also at lower temperatures [30]. In our case, the whole substrate becomes black as an effect of the working atmosphere (Ar/H_2 and zirconium getter) more than for the presence of active metals; this fact is confirmed by the blackening of zirconia isolated substrates, not in contact with the molten metal, treated under the same experimental conditions. Thus, the zirconia acts as an oxygen source following the reaction $ZrO_2 \leftrightarrow ZrO_{2-x} + x/2\ O_2$ (whose ΔG is a function of T and P_{O_2} through *"x"*) leading to the formation of Al_2O_3 at the M/C interface for CMSX486 and IN738LC. Moreover it should be remarked that the content of aluminum available for the oxidation processes in the nickel-based alloys used in this work is very high: 12.95 at.% for CMSX486 and 7.28 at.% for IN738LC.

Generally, pure nickel and cobalt do not wet zirconia [30–33]; of course, their wetting is influenced by the presence of active elements. In our case, Ni-based superalloys wet zirconia (81° angle was obtained for both CMSX486 and IN739LC alloys) but Co-based ECY768 does not (107° reported). Moreover [30], wetting of zirconia by both liquid metals and alloys is influenced by the stoichiometry of the substrate resulting in improved wetting when the substrate loses oxygen becoming black; in this case there is formation of a large quantity of Zr-metal bonds due to the larger availability of free electrons.

For almost all the systems the contact angle is reached just after a few seconds from melting, indicating that the phenomena described so far reach the equilibrium very soon. This is not the case of the CMSX486 and ECY768-mullite couples for which the final contact angle is achieved after several minutes. This fact could be explained by the phenomenon of decomposition of mullite [34–36] which occurs from the surface to the bulk, at high temperatures and low P_{O_2} leading to the evolution of SiO and O_2 and formation of α-Al_2O_3 retaining the acicular shape of mullite. The evolution of oxidizing agents leads to the formation of the thin layer of HfO_2 for CMSX486, which prevents any further oxidation, and of a thick layer of Al_2O_3 for IN738LC which prevents the evolution of the drop shape; no oxidation of ECY768 has been reported.

Moreover, for the CMSX486-mullite system, the formation of a layer of alumina also below the drop is explained by the reaction $3Al_6Si_2O_{13} + 8Al \leftrightarrow 13Al_2O_3 + 6Si$ [37] which has, at 1500 °C, $\Delta G = -748$ kJ/mol.

Conclusions

The wetting of three superalloys (CMSX486, IN738LC, and ECY768) in contact with different oxides (sapphire, polycrystalline alumina, zirconia, and mullite) has been evaluated by sessile drop experiments conducted at 1500 °C under Ar/H_2 atmosphere. The microanalysis performed on solidified samples showed that the formation of compounds at the M/C interface is dominated by the few active elements (Hf in particular but also Al and Zr) present, also at low concentrations, in the alloys. Other elements present at high concentrations, such as Cr in all the alloys or Co for Ni-based and Ni for Co-based superalloys, or at low concentrations such as Ti, W, Ta, Mo, Re did not show any effect in the formation of interfacial compounds. The lower wettability of mullite has been discussed and attributed to its partial decomposition in the low P_{O_2} experimental environment.

In general, this study clearly shows that, when trying to design new alloy compositions to improve their thermo-mechanical characteristics, a special care should be paid to control the effects that interfacial active elements could have on the behavior of the molten metal in contact with mold material.

Acknowledgements The authors wish to thank Mr. Carlo Bottino for SEM-EDS analysis and Mr. Francesco Mocellin for technical support. The authors wish also to thank Dr.Michele Di Foggia (Europea Microfusioni Aerospaziali, Italy) for supplying the superalloys and for his continuous support in this research. This work was partially funded by the FIRB-FAR MITGEA Project n° RBIP064N2X of the Italian University and Research Ministry.

References

1. Konter M, Thumann M (2001) J Mat Proc Tech 117:386
2. Donachie MJ, Donachie SJ (2002) Superalloys a technical guide. ASM Intl, Materials Park, Ohio
3. D'Souza N (2009) Mat Sci Tech Ser 25(2):170
4. Kanetkar CS, Kacar AS, Stefanescu DM (1988) Metall Trans A 19A:1833
5. Virieux XY, Desmaison J, Labbe JC, Gabriel A (1997) Mater Sci Forum 251:925
6. Jia Q, Cui YY, Yang R (2006) J Mater Sci 41(10):3045. doi: 10.1007/s10853-006-6785-3
7. Mileiko ST (2006) Curr Opin Solid State Mater Sci 9(4):219

8. Asthana R, Mileiko ST, Sobczak N (2006) Bull Polish Acad Sci 54(2):147
9. Muolo ML, Ferrera E, Morbelli L, Passerone A (2004) Scr Mater 50(3):325
10. Arroyave R, Eagar TW, Larson H (2003) Fuel Chem Div Prepr 48(1):247
11. Sciti D, Bellosi A, Esposito L (2001) J Am Ceram Soc 21(1):45
12. Eustathopoulos N, Nicholas MG, Drevet B (1999) Wettability at high temperatures. Pergamon Materials Series, Oxford
13. Liggieri L, Passerone A (1989) High Temp Technol 7:82
14. Passerone A, Ricci E (1998) Drops and bubbles in interfacial research. Elsevier, Amsterdam
15. Eustathoupoulos N, Sobczak N, Passerone A, Nogi K (2005) J Mater Sci 40:2271. doi:10.1007/s10853-005-1945-4
16. Champion JA, Keene BJ, Sillwood JM (1969) J Mater Sci 4:39. doi:10.1007/BF00555046
17. Saiz E, Tomsia AP, Cannon RM (1998) Acta Mater 46(7):2349
18. Grigorenko N, Zhuravlev V, Poluyanskaya V, Naidich YV, Eusthatoupoulos N, Silvain JF, Bihr JC (1998) In: Eustathopoulos N, Sobczak N (eds) Proceedings of 2nd high temperature capillarity conf. Foundry Research Inst., Cracow, pp 133–137
19. Champion JA, Keene BJ, Sillwood JM (1969) J Mater Sci 4:1111. doi:10.1007/BF00549852
20. Passerone A (1971) Ann Chim 61:212
21. Levi G, Scheu C, Kaplan WD (2001) Interface Sci 9:213
22. Levi G, Clarke DR, Kaplan WD (2004) Interface Sci 12:73
23. Crispin RM, Nicholas D (1976) J Mater Sci 11:17. doi:10.1007/BF00541069
24. Kurkjian CR, Kingery WD (1956) J Phys Chem 60:961
25. Sutton WH, Feingold E (1966) Mater Sci Res 3:577
26. Kritsalis P, Merlin V, Coudurier L, Eusthatopoulos N (1992) Acta Metall Mater 40(6):1167
27. Wan C, Kritsalis P, Drevet B, Eustathopoulos N (1996) Mater Sci Eng A 207:181
28. Beruto D, Barco L, Passerone A (1981) In: Vijh AK (ed) Oxides and Oxide films. M. Dekker INC, New York
29. Barin I, Knacke O (1973) Thermochemical properties of inorganic substances. Springer, Berlin
30. Durov AV, Naidich YV, Kostyuk BD (2005) J Mater Sci 40:2173. doi:10.1007/s10853-005-1928-5
31. Nikolopoulos P, Ondracek G, Sotiropoulou D (1989) Ceram Int 15:201
32. Munoz MC, Gallego S, Beltran JI, Cerdà J (2006) Surf Sci Rep 61:303
33. Sotiropoulou D, Nikolopoulos P (1993) J Mater Sci 28:356. doi:10.1007/BF00357807
34. Davis RF, Aksay IA, Pask JA (1972) J Am Ceram Soc 55(2):98
35. Grosheva VM, Panasevich VM, Boichun VYu (1968) Glass Ceram 25(3):180
36. Schneider H, Komarneni S (2005) Mullite. Wiley-VCH, Weinheim
37. Fahrenholtz WG, Ewsuk KG, Tomsia AP, Loehman RE (1996) In: Tomsia AP, Glaeser AM (eds) Ceramic microstructures. Plenum Press, New York and London